# DISCUSSIONS

# 36th INTERNATIONAL WORKSHOP ON WATER WAVES AND FLOATING BODIES

**HOST: YONGHWAN KIM**

**25-28TH APRIL, 2021**

**VIRTUAL WORKSHOP**

**SEOUL, KOREA**

Photograph: Gangneung Sea Waves of Korea, Republic of

# DISCUSSIONS

# 36th INTERNATIONAL WORKSHOP ON WATER WAVES AND FLOATING BODIES

**HOST: YONGHWAN KIM**

**25-28TH APRIL, 2021**

**VIRTUAL WORKSHOP**

**SEOUL, KOREA**

# PREFACE

The International Workshop on Water Waves and Floating Bodies is an annual meeting of engineers and scientists with a particular interest in water waves and their effects on floating and submerged bodies. In the organization and conduct of the Workshop, particular emphasis is given to the participation of younger researchers, interdisciplinary discussion between engineers and scientists, and the presentation of preliminary work before it is published elsewhere.

Since its inception, the Workshop has grown from strength to strength and annually brings together marine hydrodynamicists, naval architects, offshore and arctic engineers and other scientists and mathematicians, to discuss current research and practical problems. Attendance is restricted to the authors of submitted extended abstracts that are reviewed for acceptance by a small committee. The Proceedings of each Workshop include Introductions with background information, copies of the extended abstracts, and recorded discussions, all posted here under the page for each Workshop.

The success of the Workshops is due not only to the dedication of the participants, but also to the efforts of the host/organizers for each event and to the financial support of many government and industrial sponsors. These organizations and people are identified in each Introduction. Special sessions have been organized at some Workshops to honor individuals who have participated in the Workshops, as well as some mentors who predated the Workshops.

The IWWWFB was initiated by Professor D. V. Evans (University of Bristol) and Professor J. N. Newman (MIT) following informal meetings between their research groups in 1984. First intended to promote communications between workers in the UK and the USA, the interest and participation quickly spread to include researchers from many other countries. The first Workshops evolved from meetings of the Analytical Ship-Wave Relations Panel (H5) of the Society of Naval Architects and Marine Engineers. These were held in the United States, but frequently attended by visitors from other countries. The Introductions to IWWWFB20 (2005) and IWWWFB21 (2006) include personal anecdotes by Professors Evans and Newman regarding the historical background of the Workshops.

# Discussion Sheet

**Paper title :** Modeling fully nonlinear wave-structure interaction by an adaptive harmonic polynomial cell method with immersed boundaries

**Author(s):** C. Tong, Y. Shao, H. Bingham

**Question(s) / Comment(s):**

Many thanks for such a nice work. I have a few questions/suggestions:

1) To which variables do you apply the filter? Do you apply the filter to the free surface profile or also to the velocity potential?
2) The data in the right picture of Fig. 3 are not easy to interpret. Plotting (A-A*)/A, either in logarithmic or linear scale, would have been better.
3) Would it be possible to extend the method to deal with water impact problems with the body initially above the free surface?

**Asked by :** Alessandro Iafrati

**Answer:**

Than you that you are interested in my work.
Regarding to your questions and suggestions, here is my reply:

1) Actually, both the selective filters and optimized WLS(13,10) filters are applied to both the free surface profile and the velocity potential of the free surface.
2) Thanks for that suggestion, but I tried that and it seems not to be distinctive if we plot (A-A*)/A in linear scale.
   It has nothing different with the plot left in Figure 3. You can refer to the plot I attached below.
   If we plot (A-A*)/A in log scale, it is almost the same with the picture right in Figure 3.
3) Theoretically, it can be extended to deal with water impact or wave plunging be fore breaking as what have done in Jingbo Wang's work (A harmonic polynomi al method based on Cartesian grids with local refinement for complex wave-bod

y interactions).

However, the grid system from his is totally different as far as I know. The grid generation can be very fast in our work and very easy to implement even if in 3D scenarios. It means we can do the same things as what Wan g has done
if more techniques are added in present work. We don't do that because wa ter
impact or wave breaking problems are not our research interests currently. I f you want solve the water impact problem, as the same as other potential flow solvers, such as BEM, we need to assume a very small initial wetted surface at t=0 and start the flow from there.

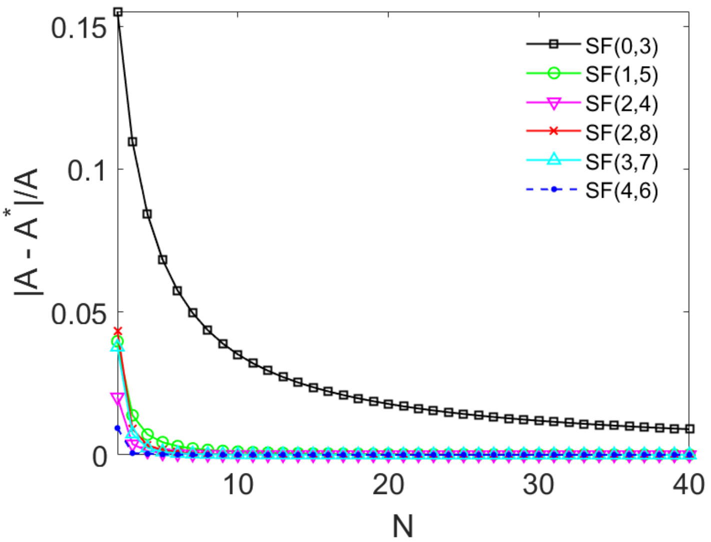


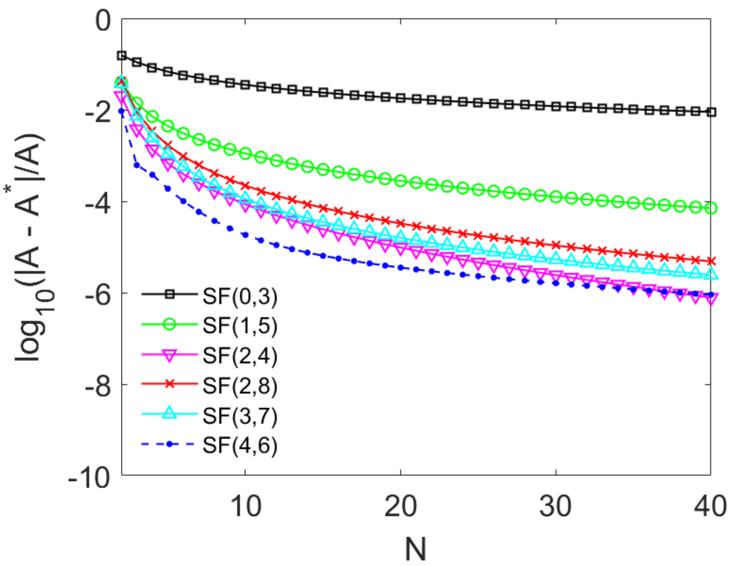

# Discussion Sheet

**Paper title: Higher order phenomena for a two-dimensional breaking wave impact on a vertical wall**
**Author(s): T. Tsaousis, I.K. Chatjigeorgiou**

**Question(s) / Comment(s):**

**Breaking wave impact can be approximated by impact of a part of the wall onto the liquid layer, which is initially at rest, in the leading order of the pressure-impulse approach. How to justify that this approach can be used in higher-order models?**

You are right, given that the physical meaning of our higher order model needs to be further examined. However, the main purpose of our presentation was to offer a novel approach to a complicated Sturm-Liouville problem in slamming theory, which has not been treated so far. At any case, the solution to the higher order problem accounts for very rapid changes in the dynamics of the impact, relatively to the leading order solution.

**Your boundary conditions on the free surface are linearized but imposed on the actual position of the free surface. Why can we do this**

This approach is analogous to the linearization process of the free surface boundary conditions on regular wave hydrodynamics. The corresponding methodology in regular wave hydrodynamics is: 1) nonlinear kinematic and dynamic boundary conditions imposed on the real free surface position, 2) linearization of the conditions (due to the small steepness of the wave) still imposed on the real free surface position and 3) Taylor series expansion around the still water level. At any case, the higher order b.v.p. -as well as the leading order- are solved at a steady domain, bounded from above by the still water level.

**Asked by: A. Korobkin**

# Discussion Sheet

**Paper title: Flow separation model for the water entry of smoothly curved bodies**
**Author(s): A.D. Buono, A. Iafrati, G. Bernardini**

**Question(s) / Comment(s):**

How are the pressure distribution in the place of separation and the quality of the body surface (hydrophobic?) important for accurate estimation of the position of the separation points?

**Asked by : A. Korobkin**

**Answer:**

Thank you for your question.
The present model does not use directly the pressure to fix the separation point. The idea behind the proposed model is that if the fluid particle has to move along a curved contour there should exist a pressure gradient which is proportional to the local curvature. For a convex body shape the pressure gradient is oriented inwards the fluid domain.
At the external surface of the thin jet the pressure is zero, and thus the pressure at the body side should be negative for the flow to be attached. As a consequence, the separation based on the negative pressure criterion would predict the separation of the thin spray in all conditions. It is expected that the kinematic criterion could be more general.

The quality of the body surface has no effects on the present model. Other important aspects, such as viscosity and surface tension, are also neglected.

# Discussion Sheet

**Paper title: Wet and dry modes of complex structures in impact problems**
**Author(s): T. Khabakhpasheva, A. Korobkin**

**Question(s) / Comment(s): If I understand correctly, your analysis would be equivalent to the infinite frequency limit of the wave problem. Would this be useful in the context of approximating a ship by a beam, and calculating the relevant flexible mode shapes and eigenfrequencies?**

**Asked by: Harry Bingham**

**Answer:**

Our analysis is for processes of short duration such as impact on a floating elastic plate and entry of a slightly curved plate into water. Gravity plays minor role in these violent problems of hydroelasticity. Indeed, our analysis can be extended and applied to ship whipping (but not springing), when the ship is modelled as a 1D non-uniform beam with free-free ends subject to wave impact. To estimate whipping, we need “wet” modes of the ship and the corresponding wet frequencies, which can be obtained by our approach after further development.

# Discussion Sheet

**Paper title : Sloshing and scattering in shallow water**
**Author(s): D.V. Evans**

**Question(s) / Comment(s):**

**Your new solution applies to a bed whose sides meet the surface vertically but shallow water theory applies in the limit where vertical accelerations are ignored. Can you comment on how this contradiction might be resolved**

**Asked by : Richard Porter**

**Answer: You are quite right of course despite many papers having been written which clearly violate the shallow water equation. One way forward, short of using full linear theory, would be to use one of the modified shallow water equations whose development you have contributed to in the past. However it is not clear that they would yield the explicit result for the bottom shape that I have shown here using the simpler equation.**

**35th International Workshop on Water Waves and Floating Bodies**

**April 25-28, 2021**

# Discussion Sheet

**Paper title :** Analytical representation of flows due to arbitrary singularity distributions for wave diffraction radiation by offshore structures in water of finite depth

**Author(s):** H. Wu, J. He, F. Noblesse

**Question(s) / Comment(s):**

Thank you for very nice work on difficult subject. Here are my questions:

1. What is the role of $\mu^*$ in the computation of local and wave components? It seems that this parameter is introduced to facilitate the numerical computation.

2. If the final results obtained by different $\mu^*$ are the same, why the total wave components are decomposed into the local and wave parts?

**Asked by :** Young-Myung Choi, Bureau Veritas, Paris, France

**Answer:**

Thank you for your questions.

1. The parameter $\mu^*$ controls the width of the `dispersion strips' related to the localizing function introduced in the analysis. It is introduced to make the local-flow and the wave components smooth. Although both the local-flow and the wave components include $\mu^*$ and depend on $\mu^*$, the total flow potential is independent of $\mu^*$. We can see from the figures that in the special case $\mu^* = 0$, which corresponds to the classical decomposition, the local-flow and the wave components are not smooth, although the sum of them is smooth. For $\mu^* = 20$, the local-flow potential includes near-field waves. Thus, $\mu^*$ should not be chosen too small or too large. The numerical study about the influence of $\mu^*$ on flow potentials and on amplitude functions shows that the choice $\mu^* \approx 0.5$ is satisfactory.

2. The total flow potential is given by a singular double Fourier integral, which is difficult to evaluate. Both the local-flow and the wave potentials are given by regular integrals, which are much better suited for practical numerical evaluation.

# Discussion Sheet

**Paper title : Effects of water depth and nonlinearity on the wavefront**

**Author(s): Y. Xu, K. Zheng, B.B. Zhao, R.P. Li ,W.Y. Duan, M. Hayatdavoodi, R.C. Ertekin**

**Question(s) / Comment(s):**

Some articles already give wave front points, can you give wave front point information here and compare wave front components?

**Asked by : Xiaobo Chen**

**Answer:**

At linear theory, the wave front points propagate forward with group velocity in infinite water depth . In the transient wave, we can give the result of the wavefront time history, but can not give the definition of the wavefront point analytically.

**Question(s) / Comment(s):**

What kind of wave-making boundary are you using?

**Asked by : Harry Bingham**

**Answer:**

The fully nonlinear stream function wave theory is used at the wave maker.

# Discussion Sheet

**Paper title : Linear motions of fish tanks**

**Author(s): J.N. Newman**

**Question(s) / Comment(s): It's interesting how the addition of what seems to be a relatively small flotation ring introduces a dramatic pitch resonance into the system, but otherwise tends to reduce the response. How significant do you think this resonance might be in practice?**

**Asked by : H.B. Bingham**

**Answer: In practice this low-frequency resonance would certainly be affected by nonlinear effects, and also by mooring restraints. Perhaps the most obvious nonlinearity is the effect of a small pitch angle on the hydrostatic restoring moment of the float.**

# Discussion Sheet

**Paper title: Water wave scattering by a submerged inclined poroelastic plate**
**Author(s): M. Singh, R. Gayen**

**Question(s) / Comment(s):**

**The coefficient J in the relation for R and T is very interesting. It peaks at G=0.5. What does this G=0.5 means for the plate? This J reduces the sum |R|+|T|. Which term of this sum is most reduced?**

**Asked by: A. Korobkin**

**Answer:**

**Here $G$ denotes porosity parameter. Its expression is given by,**

$$G = \frac{\gamma\,(f_r + i\,f_i)}{K\,d\,(f_r^2 + f_i^2)}\ ,$$

**where, $\gamma$ denotes the porosity of the plate, $f_r$ denotes resistance force coefficient, $f_i$ denotes inertial force coefficient and $d$ denotes the thickness of the plate.**

**From figure 3(b), it may be observed that as the real part of $G$ increases $J$ increases. $J$ is maximum for $G = 1$. However, keeping the real part of $G$ fixed, if the imaginary part of $G$ is increased it may be observed that J gradually decreases. Thus, it may be concluded that the increment in the real part of $G$, i.e., the resistance force, is responsible for increment in energy dissipation. This is also visible from the energy identity given by,**

$$|R|^2 + |T|^2 = 1 - J\,,$$

where, $J = 2(KL)\ Re(G) \int_{-1}^{1} \left| \sqrt{1-t^2} \sum_{n=1}^{M} a_n\, U_{n-1}(t) \right|^2 dt.$

**The following table also strengthens our claim that with the increase in $Re(G)$, $J$ increases.**

| $G$ | $\|R\|$ | $\|T\|$ | $\|R\|^2 + \|T\|^2$ | $J$ | $1-J$ |
|---|---|---|---|---|---|
| 0.3 | 0.2254 | 0.9233 | 0.9033 | 0.0967 | 0.9033 |
| 0.5 | 0.2229 | 0.8865 | 0.8355 | 0.1644 | 0.8356 |
| 0.7 | 0.2161 | 0.8639 | 0.7930 | 0.2069 | 0.7931 |
| 0.9 | 0.2060 | 0.8460 | 0.7582 | 0.2418 | 0.7582 |
| 1.1 | 0.1941 | 0.8367 | 0.7378 | 0.2623 | 0.7377 |

**Here it may be noted that with the increase in $G$, both $R$ and $T$ decreases resulting in the decrease in $|R|^2 + |T|^2$ .**

# Discussion Sheet

**Paper title :** Numerical and experimental investigation of dam-break flow against a vertical cylinder
**Author(s):** C. Hu, M. Karma, S. Watanabe

**Question(s) / Comment(s):**

Thank you for the interesting work and presentation. We are studying the same problem by use of the shallow-water GN equations. Two questions:

- In your test cases, there is no water downstream the gate. In such cases, we have found that the form of the bore changes as it propagates downstream. Hence, the loads on the cylinder would change depending on the distance of the structure from the gate. How did you choose the position of the cylinder in your study?
- Can you comment on the effect of viscosity and turbulence on the bore-induced pressure on the cylinder and the downstream wall?

**Asked by :** Masoud Hayatdavoodi

**Answer:**

Thank you very much for your question.

- Yes, we also observed that the bore shape changes during its propagation. I agree with you that the influence of the distance of the structure from the gate may influence the loads on the cylinder. The position of the cylinder was chosen to place near the downstream wall.
- From our experience with CFD simulation, turbulence model has a great influence on pressure calculation. For the unstructured mesh FVM code, we have tested several models, including k-ω, k-ε, and LES. We found k-ε model gives best impact pressure prediction on the studied case.

# Discussion Sheet

**Paper title : Numerical Simulation on the Slow-drift Motion of a Semi-Submersible Platform Considering Mooring Effects**
**Author(s): BW Nam, MG Seo, SY Hong**

**Question(s) / Comment(s):**

1. What is the oscillation frequency of the drift force? Zero frequency or low frequency according to the wave spectrum?
2. Is the drift force for fixed body or moving body?

**Asked by : Bin Teng**

**Answer:**

1. In this study, the oscillation frequency is in the range of 0.05 rad/s to 2.0 rad/s. For the drift force computation, Newman's approximation is applied.

2. The drift force is calculated for the moving body considering 6-DOF motion of the semi-submersible platform.

# Discussion Sheet

**Paper title : A flexible multi-torus solar island concept**
**Author(s): T Kristiansen, M V Sigstad, J Winsvold, O Rablias, OM Faltinsen**

**Question(s) / Comment(s):**

Have you checked the influence of restoring matrix for RAO? During the oscillatio n, the mean width of water-plan should be smaller than the diameter of the pipe.

**Asked by : Bin Teng**

**Answer:**

Your question is very relevant. In the case that there is substantial relative vertical motion between the torus and the incident wave, i.e when the relative motion is comparable in size to the cross-sectional radius of the torus, the varying cross-section/low draft is an effect that one should think matters.

Based on previous investigations of a single flexible torus, we believe that this may be a cause of significant *higher-harmonic* vertical accelerations of the torus.

However, the RAOs are based on the *wave-frequency* motions only. For the wave-frequency motions, the varying draft seems not to matter, at least for the tested wave frequency range. We base this statement on the figure below. There, RAOs in heave for the outer torus are presented for two wave steepnesses $H/\lambda$. The left figure represents the lowest wave steepness $\frac{H}{\lambda} = 1/60$, while the right represents the highest wave steepness $\frac{H}{\lambda} = 1/30$. The underscore "_m1" in the legend refers to tests with membrane deck, so please compare the yellow curve in the left plot and the red curve in the right plot. We see that the RAOs are practically equal for the two wave steepnesses. This is so, even though the numerical simulations (by WAMIT) predict a non-negligible relative motion, in the order of half the cross-sectional radius. The largest relative motion occur for the range of non-dimensional wave number $kR_1 = 3 - 5$. In the steepest wave case, the predicted relative motion is twice that in the lower wave steepness case. If the varying cross-section mattered, one should expect to see differences in the RAOs, something we don't. The causes of the irregularities not caused by tank wall reflections thus remain to be explained.

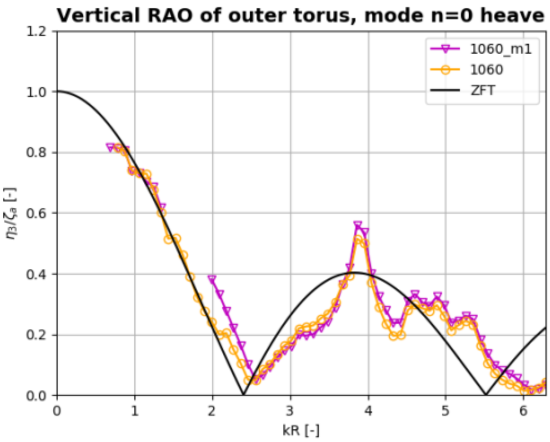


(a) Steepness $H/\lambda = 1/60$

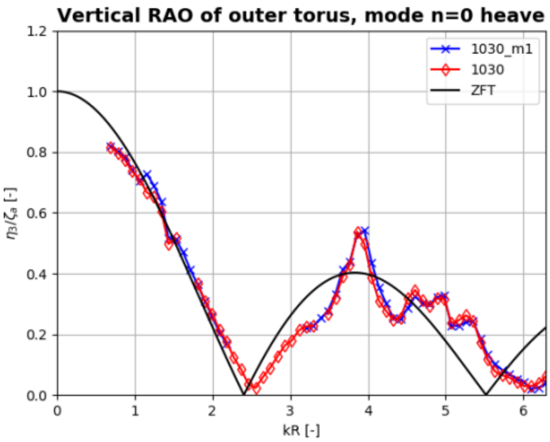


(b) Steepness $H/\lambda = 1/30$

**36th International Workshop on Water Waves and Floating Bodies**

**April 25-28, 2021**

# Discussion Sheet

**Paper title : Numerical study on freely floating vertical cylinders by full nonlinear three-dimensional potential-flow numerical wave tank**

**Author(s): SJ Kim, MH Kim**

**Question(s) / Comment(s):**

1. For the third order force on the truncated cylinder (Fig 2), have you compared the heave component?
2. For the RAO (Fig. 3), it seems that there is a resonant frequency between KR=0.2-0.3. Have you done more calculation in these wave number range to capture the peak?

Remind:

The following seems to be a mistyping:

'image sources are located with respect to mean water level and flat bottom'

Eq. 3 seems that the image sources are located with respect to the center plan of the tank and flat bottom'

**Asked by : Bin Teng**

**Answer:**

Thank you for the comments.

1. Yes, we have done. Following two figures show the various frequency components of vertical wave loads acting on the truncated vertical cylinder (h/R = 10.0, d/R=1.0; h=water depth, R=radius of a cylinder, d=draft of a cylinder). Following two figures show the various frequency components of vertical wave loads acting on the truncated vertical cylinder. In the figures, the results of 'Diffraction' are from WAMIT v. 6.1s and Teng and Kato (2002) estimated the third order wave loads by perturbation-based frequency domain analysis.

   The present fully nonlinear NWT results are generally in good agreement with the other independently computed results. With regard to the third-order vertical forces on the truncated cylinder, although their general trends are close, the agreement in magnitude is worse than the horizontal wave loads but "which result is more correct?" is not clear since the third-order perturbation theory itself also contains several numerical difficulties such as high-order derivatives on the body surface including corners.

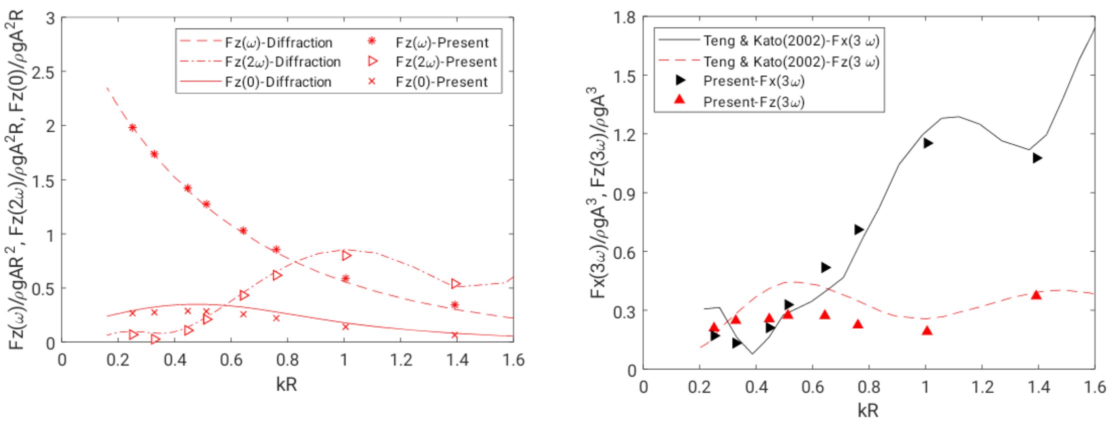


<First order, second order and third order wave loads>

2. Unfortunately, the reference paper did not provide those resonance-peak values. The resonance peaks are exaggerated by perturbation-based potential theory and fully-nonlinear simulations can somewhat limit those peaks, as shown in the results. We have added the results at kR=0.25 and they have a good agreement.

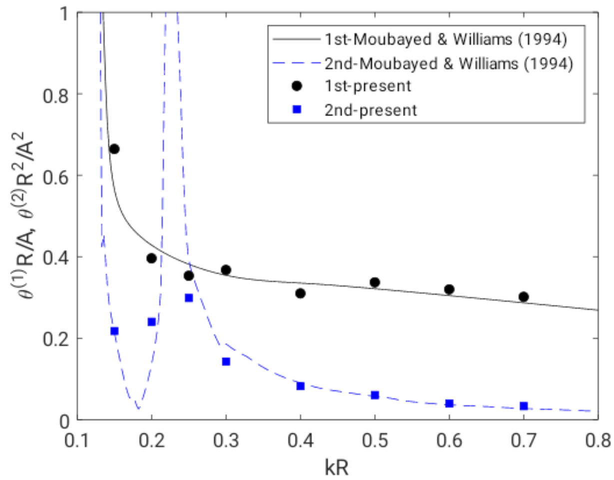


<First order and second order pitch motion RAO>

# Discussion Sheet

---

**Paper title: Ship-driven mini-tsunamis at a depth change: field measurements and theory compared**
**Author(s): J. Grue**

---

**Question(s) / Comment(s): Only a comment, John, when I thought there was more time and that your wonderful talk deserved more response:**

**when I first visited the UiO Math Dept a long time ago (40 years!) I was impressed to find that there was a small wave tank in the basement. Now it is even more impressive: you have a full-scale wave basin too!**

**Asked by: J. Nicholas Newman**

**Answer:**

Thanks, Nick, and a good thing in addition, is that the Oslofjorden ship tsunami experiment attracts much more public attention!

# Discussion Sheet

**Paper title :** **On head-on collision of the depression internal solitary wave and the elevation interna solitary wave**

**Author(s): T.Y. Zhang, Z.H. Wang, Z. Wang, B.B. Zhao, W.Y. Duan**

**Question(s) / Comment(s): From your results, I could not identify any interaction between the surface and the internal solitary waves. Did I miss something? Under what real-world conditions would you expect to see significant interaction between these waves?**

**Asked by : Harry Bingham**

**Answer:**

**Under real-world conditions, no one has observed this phenomenon yet. However, under the conditions we set, both internal solitary waves and solitary waves exist in the real ocean. In Fig 1, Alford et al. (2015) show the evolution of internal waves in the South China Sea. The area of the red line column is the selected area for our calculation. It is reasonable to set the whole water depth 1000m. As shown in the Fig 2, Huang et al. (2015) observed internal solitary waves with the amplitude of 240m. Thus, it is reasonable to take the amplitude of internal solitary wave as 50m.**

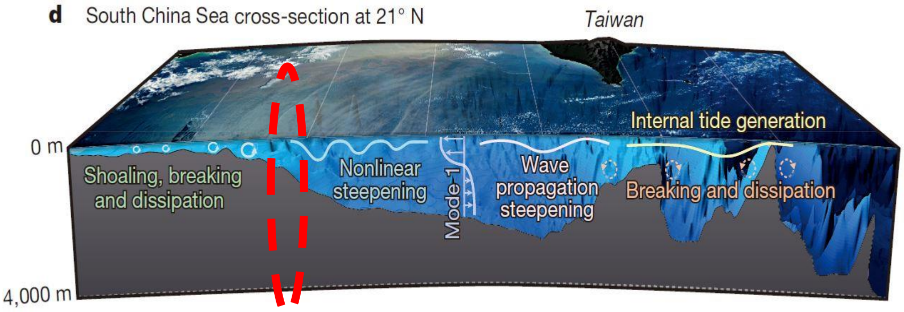

Fig 1 Evolution of internal solitary waves in the South China Sea (Alford et al, 2015)

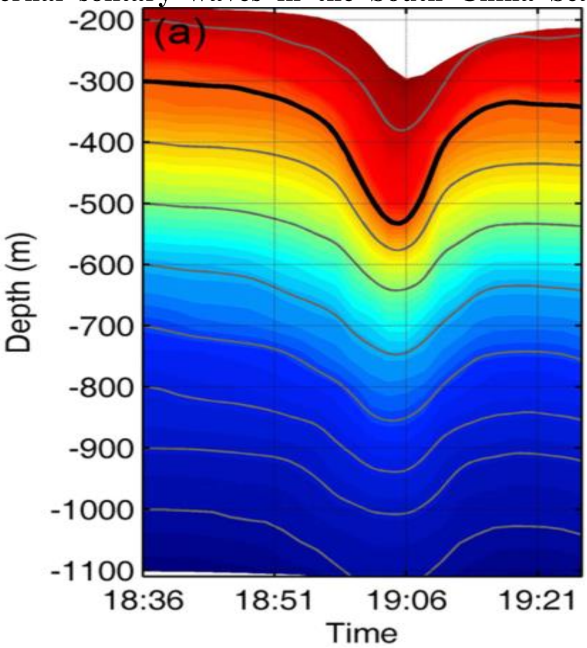


Fig 2 240m internal solitary wave in South China Sea (Huang et al., 2016)

**Meanwhile, the height of tsunamis can reach 50m. For example, in Fig 3, the height of Loenvatnet tsunami can reach 70m. More information about the height of tsunamis can refer to the websites we show below. Thus, we considered a possible extreme situation.**

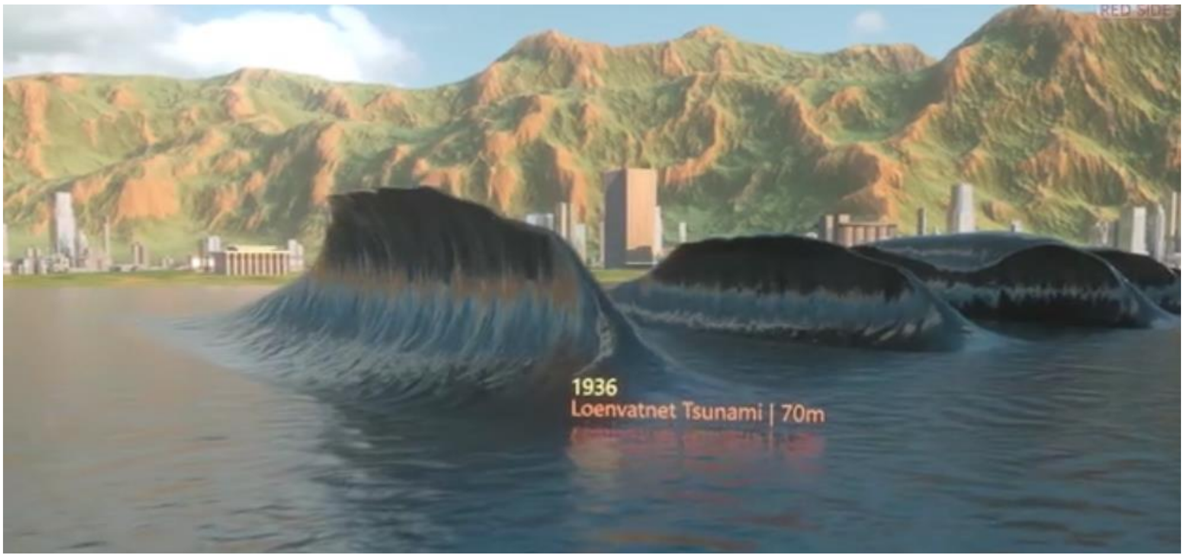


Fig 3 Loenvatnet Tsunami (1936)

**For the interaction between the surface and the internal solitary waves. In order to verify whether the interaction exists, we compare the results of linear superposition with the present numerical results. Fig 4 shows the results on the symmetry interface elevation during the collision. There are obvious differences between the results of**

**linear superposition with the present numerical results, which indicate the existence of interaction.**

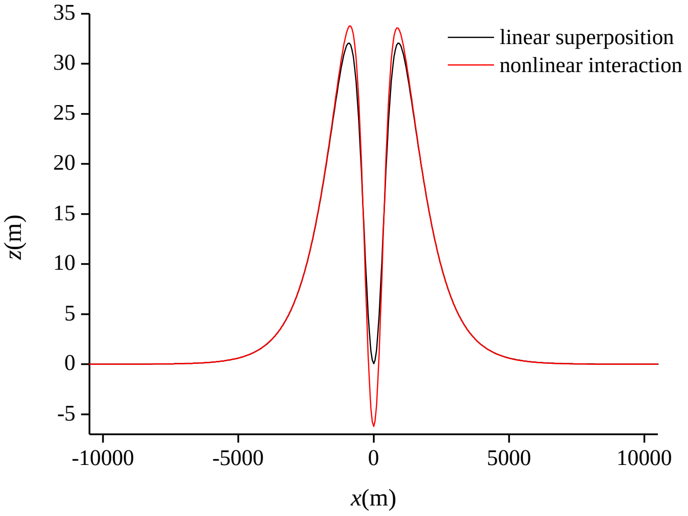


**Fig 4 The results of linear superposition VS the present numerical results**

**Finally, we refer to the literature and website attached to the following part.**


**[1] Alford M.H., Peacock T., MacKinnon J.A., et al. The formation and fate of internal waves in the South China Sea[J]. Nature, 2015, 521. 65–69.**

**[2] Huang X.D., Chen Z.H., Zhao W., et al. An extreme internal solitary wave event observed in the northern South China Sea[J]. Scientific Reports, 2016, 6 (1): 30041.**

**[3] https://www.allthingsnature.org/what-was-the-tallest-tsunami-ever-recorded.htm**

**[4] https://m.youtube.com/watch?v=DI9Y24SKPEg**

**36th International Workshop on Water Waves and Floating Bodies**

**April 25-28, 2021**

# Discussion Sheet

**Paper title :** **Phase locking phenomenon in the modulational instability of surface gravity waves**

**Author(s): S. Liu, T. Waseda, X. Zhang**

**Question(s) / Comment(s): It's not really clear to me what this phase locking implies in a practical sense. Can you say more about why this is significant in the context of extreme wave events?**

**Asked by : Harry Bingham**

**Answer:**

Dear Prof. Bingham,

Thanks for your comments. The extreme wave crests are formed by the superposi tion of wave components with different frequency. The phases of each wave compo nents play a significant role in this superposition. Specifically, if the crest of one w ave overlaps with the crest of another, a larger wave is generated, and the crest hei ght is depended on the amplitudes of these two waves. In the contrast, if the crest of one wave overlaps with the trough of another, the crest height is significantly re duced.

As for the special three-wave system considered here where the modulational ins tability is triggered, the ideal maximum wave crest is achieved as the plane wave a nd sidebands reach their peaks at the same time. Assuming the carrier wave $a_1$cos $(k_1 x + \varphi_1)$ and upper sideband $a_3\cos(k_3 x + \varphi_3)$ reach their crests at $x = x_0$, we h ave

$$\begin{cases} \cos(k_1 x_0 + \varphi_1) = 1 \\ \cos(k_3 x_0 + \varphi_3) = 1 \end{cases}$$

Considering the interaction phase is locked $2\varphi_1 - \varphi_3 - \varphi_4 = \pi/2$, it can be derived that

$$\cos(k_4 x_0 + \varphi_4) = 0$$

This implies that when the crests of carrier wave and upper band are overlapped w ith the zero point of the lower band. Therefore, the ideal maximum crest height ca nnot be achieved as the interaction phase is locked. In conclusion, we think the a nalysis of the wave phase is helpful to understand the generation of large wave in the modulational wave train.

# Discussion Sheet

**Paper title :** Influence of initial wave steepness of modulated wave trains on the maximum crest height

**Author(s):** H. Houtani, T. Waseda, H. Sawada

**Question(s) / Comment(s):**

Many thanks for such a nice work and for the very clear presentation.

I have a simple question. It is not clear to me if the analyses conducted starting from slide 14 are based on the HOSM results or on the experimental data. This is because based on slide 11 wave breaking is found for steepness beyond 0.108 and thus, I would expect, the results in the figure of slide 17 for steepness beyond 0.108 should be much different. Moreover, in case of breaking, the results in terms of spectral broadening after the breaking should be much noisier.

Concerning the breaking and post-breaking behavior, we performed two-fluids numerical simulation of a similar problem, albeit using higher steepness, and were able to go beyond the breaking. The results show that the breaking process lasts about 10 wave periods and that at the end of the breaking process the spectrum remains nearly frozen. Of course, a large portion of the energy, about 25%, is dissipated. The results also indicate that in some cases the maximum steepness continue to grow for a while after the breaking starts.

De Vita, Verzicco, Iafrati (2018) Breaking of modulated wave groups: kinematics and energy dissipation processes, Journal Fluid Mechanics, vol. 855, 267-298.

**Asked by :** Alessandro Iafrati

**Answer:**

Thank you for your question.

The analyses conducted starting from slide 14 are based on the HOSM simulation results; in the regime of potential theory assuming single-valued free-surface profiles. The wave profiles in the HOSM simulation with the initial steepness larger than 0.108 were still single-valued at the timing of the maximum crest heights, although wave breakings were observed in the physical experiment in such conditions. Therefore, as you pointed out, the analysis results of spectral broadening (including the figure on slide 17) would differ compared with the physical experiments.

Thank you for sharing the interesting work of your group addressing the breaking and post-breaking wave behavior. In our HOSM results, the wave spectrum varied continuously in time before and after the timing of the maximum crest height. However, the spectrum remained nearly frozen during the breaking process in your CFD results. The comparison of these results indicates the significance of the wave breaking on the quasi-resonant interaction.

# Discussion Sheet

**Paper title :** Influence of initial wave steepness of modulated wave trains on the maximum crest height

**Author(s): H. Houtani, T. Waseda, H. Sawada**

**Question(s) / Comment(s):**

**The HOS method does not normally account for wave breaking, and in fact breaks down somewhat before the steepest possible stable wave. Can you explain how you have managed to compute cases with wave breaking using this model?**

**Asked by : Harry Bingham**

**Answer:**

Thank you for your question.

The following anti-aliasing filter (proposed by West et al. (1987)) was applied in th e HOSM simulation:

$$|k| < \frac{N_x}{M+1} \mathrm{d}k$$

where $k$, $\mathrm{d}k$, $N_x$ and $M$ denote the wavenumber, the wavenumber interval, the num ber of nodes, and the order of nonlinearity, respectively. This low-pass filter remove s the energy of high-wavenumber components in the vicinity of a wave-breaking ti ming, and accordingly, the computation continued beyond the breaking event (c.f., T anaka (2001), Tian et al. (2008)).

- West, B. J., Brueckner, K. A., Janda, R. S., Milder, D. M., & Milton, R. L. (1987). A new

numerical method for surface hydrodynamics. Journal of Geophysical Research: Oceans, 92(C11), 11803-11824.
- Tanaka, M. (2001). A method of studying nonlinear random field of surface gravity waves by direct numerical simulation. Fluid Dynamics Research, 28(1), 41.
- Tian, Z., Perlin, M., & Choi, W. (2008). Evaluation of a deep-water wave breaking criterion. Physics of Fluids, 20(6), 066604.

# Discussion Sheet

**Paper title : Acoustic-gravity wave generation as a result of bottom oscillations of compressible ocean**
**Author(s): Das & Meylan**

**Question(s) / Comment(s):**

I wonder if you are aware of the work

Gravity waves and acoustic waves generated by submarine earthquakes
TOKUO YAMAMOTO
Soil Dynamics and Earthquake Engineering, 1982, Vol. 1, No. 2 75

which appears to be same problem that you are looking at.

**Asked by : Richard Porter**

**Answer:** Thank you for pointing out the paper. Yes, we are aware of the work. In fact, we are trying to solve a more generic problem based on the solution process developed by Yamamoto (1982). It is a mistake on our part that the citation was missed in the submitted abstract. We did not realize it until it was asked during the presentation.

# Discussion Sheet

**Paper title :** **Numerical analysis of wave-induced unsteady pressure on ship-hull surface**

**Author(s): K. Yang, B.S. Kim, Y. Kim, M. Kashiwagi, H. Iwashita**

**Question(s) / Comment(s):** I find it very interesting that through these detailed measurements and CFD calculations you can show that the vast majority of the added resistance forces seem to come from relatively small areas of the hull located near the bow. In particular, there are large effects from the region above the still water level. Even so, linear theory tends to give very good predictions of the total added resistance. Can you comment on this?

**Asked by : Harry Bingham**

**Answer: The added resistance is a mean quantity and it can be calculated solely based on a linear solution. We have derived the separate formulation for the added resistance and the waterline integration of relative wave height is a major "positive" contribution to the added resistance. It can be visualized as shown in our research. It should be noted that if a ship has relatively large flare angle and the amplitude of incident wave increases, then the linear theory will provide relative less accurate solutions.**

# Discussion Sheet

**Paper title : Moving load in an ice channel with a crack**
**Author(s): L Zeng et al**

**Question(s) / Comment(s):**

I wonder how common ice channels are. Wouldn't it be more realistic to consider an open ocean? I think it would be possible to extend your method to this case. Also you might consider asymmetric loads which should be possible also.

**Asked by : David Evans**

**Answer: Thank you for your questions. Ice channels can be found in northern river in winter time. Sometimes, the width of the river is not wide enough, so the influence of the channel walls will be more obvious. In addition, if we do experiment in ice tank, the effect of channel walls should be considered due to the narrow tank. Thus, we should know how the channel walls affect the response of ice, and how far is the load from the channel walls to ignore the influence of the channel walls. Then we can say, in some condition, the problem can be regarded as a load moving on open ocean covered by ice sheet.**

**Thank you for your suggestions. Our method can be extended to the case that load moving on open ocean covered by ice sheet. But we have not done it yet. The asymmetric case have been considered But the results is not finished yet, s o it was not shown in the workshop.**

# Discussion Sheet

**Paper title:** Moving load in an ice channel with a crack

**Author(s):** (Zeng L.D., Korobkin A.A., Ni B.Y., Xue Y.Z.)

**Question(s) / Comment(s):**

In your numerical results, max W (U) are constant around the critical speed for the second mode. It may be possible because \tau is too big.
Did you calculate the distribution of w for small \tau with U slightly higher and slightly less than U_critical? What does change when U passes through U_critical?

Additional comments – The second critical speed corresponds to the long wave limit (is it right?), which is close to the critical speed for the same problem with unbounded plate. Maxima and minima on the curves for deflections and strain demonstrate that other critical speeds are less important than the critical speed for the long wave limit.

**Asked by: Tatiana Khabakhpasheva**

**Answer:**

Thank you very much for your question. Yes, we calculate the distribution of w for smalle \tau with U slightly higher and less than the critical speed of the second mode. For example, U=15 m/s and 16 m/s. Please see the results in figure 1 and 2. For U=15 m/s, it is seen that there are one wave across the channel, which mainly caused by the first mode. For U=16 m/s, it is seen that there are two wave across the channel, which mainly caused by the second mode.

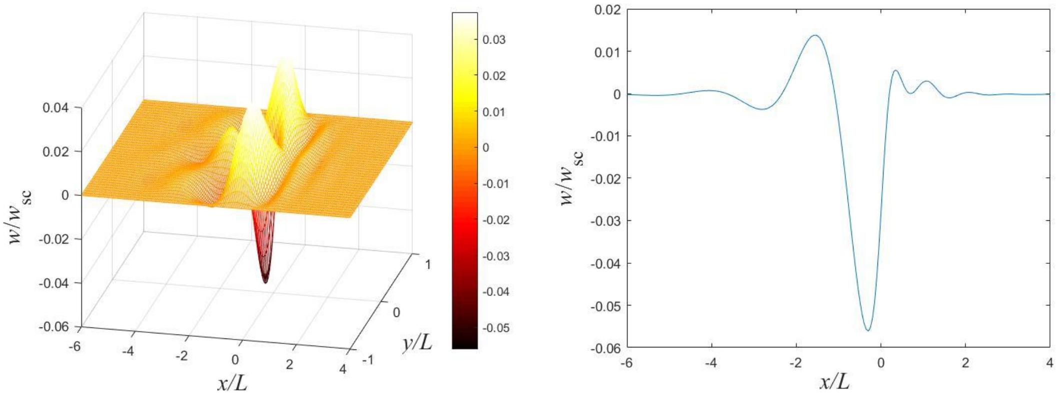


**(a) 3D wave form** **(b) Longitudinal profile**

**Fig. 1 Ice deflection for U=15 m/s**

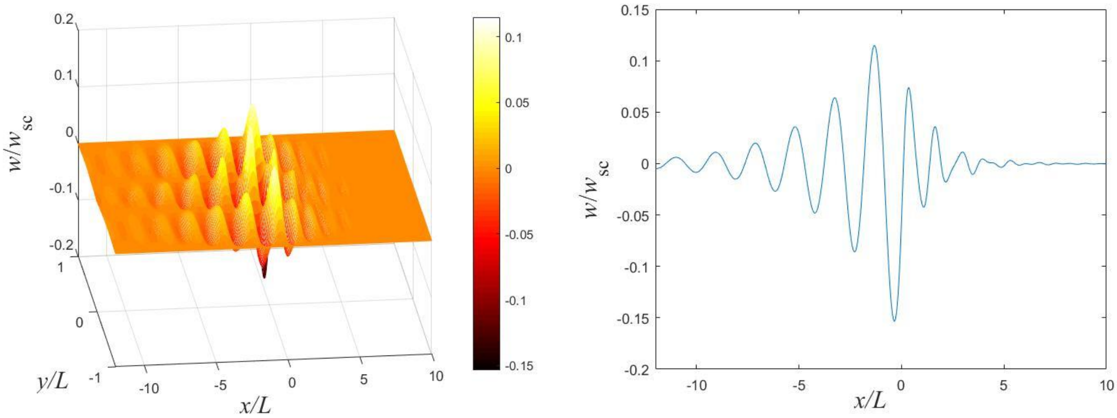


**(a) 3D wave form** **(b) Longitudinal profile**

**Fig. 2 Ice deflection for U=16 m/s**

Yes, the second critical speed corresponds to the long wave limit. But I am not sure whether the width of the channel will affect this speed. I shall check it later and then see the effect of width of channel on the second critical speed.

# Discussion Sheet

**Paper title :** **Beneficent features of Green's function with viscous effect**

**Author(s): X.B. Chen, Y.M. Choi**

**Question(s) / Comment(s):** In your comparison between the 'new' and the 'old' panel methods, the old method shows rather oscillatory added mass and damping coefficients which don't compare very well with the experiments. However, you've discussed a number of differences between the new and the old method, can you identify which changes are most important for the improvement? In particular, is it mostly related to the formulation (NK vs. double-body) or the numerical methods?

**Asked by : Harry Bingham**

**Answer:**

Yes. We mention the classical panel method based on the Neumann-Kelvin approach with inviscid Green's function as "Old BIE" which is written on the ship hull only including the waterline integral, and the present method based on the linearization over ship-shaped stream (double-body flow) with Green's function with viscous effect as "New BIE". In the New BIE, we have not only the integral on ship hull without waterline integral, but also that on the free surface in the vicinity of the hull, and the equation applied on the waterplane inside the ship to ensure the zero-potential outside the fluid domain so that any irregularity associated with integral equation of Fredholm type is removed. We would like to precise which Green function and where the BIE is used in the below table:

| BIE Type | Green Function | Where | Remark |
|---|---|---|---|
| Old BIE(H) | Inviscid | Hull | |
| Old BIE | Inviscid | Hull, Waterline | Neumann-Kelvin |
| H-BIE | Viscous | Hull | |
| W-BIE | Viscous | Hull, Waterplane | |

| | | | |
|---|---|---|---|
| T-BIE (New BIE) | Viscous | Hull, Waterplane, Free surface | Double-Body |

Computed radiation coefficients for S60, $C_B$=0.7 for Fn (Froude number) = 0.2 are compared with experimental results in below figures.

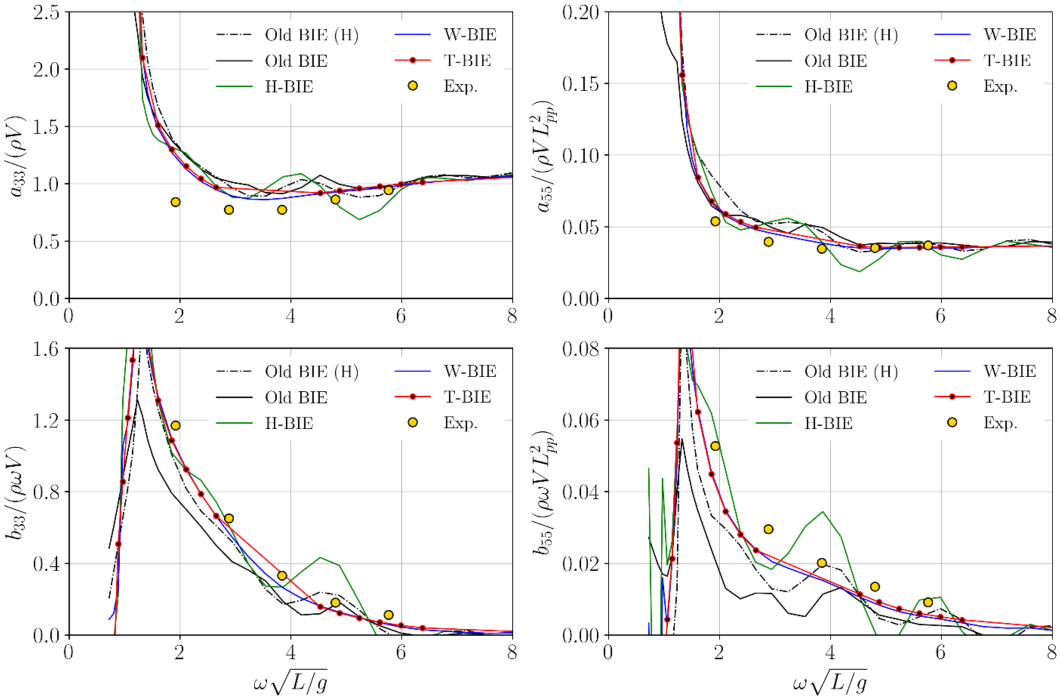


**Fig. 1** Heave and pitch added masses and radiation damping

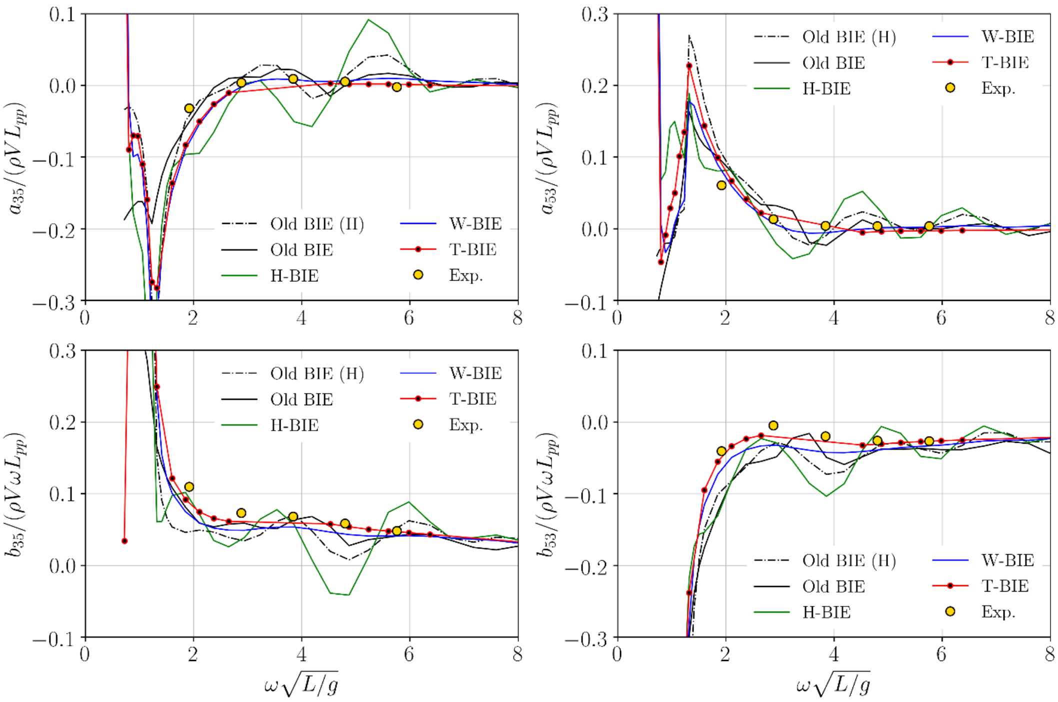


**Fig. 2** Coupled heave-pitch added masses and radiation damping

The computed radiation coefficients from Old BIE (H), Old BIE and H-BIE, are all oscillatory around experimental results. Furthermore, results with Old BIE (H) and H-BIE are worst since they are not consistent, although Green's function with viscosity is used in H-BIE. Introducing the waterplane (W-BIE) gives better results for radiation coefficients compared with Old BIEs and H-BIE, especially for pitch-motion related radiation coefficients. We infer that the irregular phenomenon occurs for all frequency in the forward speed problem because the infinite number of wavenumber is obtained from the single frequency from the dispersion equation. Therefore, ensuring the zero-potential inside of ship hull removes this irregular phenomenon, which we call "irregular wavenumber phenomenon" for forward speed problem. Consideration of free surface integral (T-BIE) gives the best results for coupled heave-pitch radiation coefficients, especially for radiation damping. In brief, we would like to summarize that all of items are critically important to get satisfactory results for forward speed problem.

- New BIE based on the linearization around the ship-shaped stream (DB flow);
- Imposing the zero-potential condition inside the ship hull (on the waterplane);
- Green's function with viscous effect and its analytic integration over flat panels.

# Discussion Sheet

**Paper title :** **Towards an efficient 3D numerical wave tank using the harmonic polynomial cell methodwith adaptive grid refinement**

**Author(s): F-C Hanssen, M.Greco, J.B. Helmers, Y.S. Shao**

**Question(s) / Comment(s):** When you apply an immersed boundary strategy together with a locally refined mesh, you will have to re-generate a large part of your system matrix at every time step. How does this affect the efficiency of your iterative solution scheme? What kind of scaling do you get for your solution effort with increasing numbers of grid points?

**Asked by : Harry Bingham**

**Answer:** We have spent a significant effort developing efficient algorithms to build the matrix equation system. Qualitatively, we have observed only a moderate increase in the time used to build the coefficient matrix when we use adaptive grid refinement compared to using a single uniform grid.

When we use local grid refinement, it is not evident that the scaling as a function of grid nodes is the most relevant since a certain accuracy of the solution can be achieved with fewer nodes. We have therefore instead chosen to plot the error of different solution variables versus the CPU time of the iterative solver in Figure 6 in our abstract. However, it is indeed reasonable to assume that the scaling is somewhat influenced by both the immersed boundary modelling and the adaptive grid refinement.

We would welcome suggestions on alternative ways to measure the scalability of our iterative solver, since the time used to estimate the preconditioner matrix is significant compared to the total solution time for large problems.

**Follow-up comment by Harry Bingham:** From a practical point of view, in my opinion, the most relevant measure of scalability is to fix the resolution (and grid refinement strategy) for a small problem, say 5 by 5 wave lengths. Then, increase the problem size to 10 by 10, 20 by 20, etc., and check the scaling of the effort.

# Discussion Sheet

---

**Paper title :** Towards an efficient 3D numerical wave tank using the harmonic polynomial cell method with adaptive grid refinement

**Author(s):** F-C Hanssen, M.Greco, J.B. Helmers, Y.S. Shao

---

**Question(s) / Comment(s):** I compliment you on the progress and promise that your works shows for the HPC method. I would like to ask if you think there is any advantage to anisoptric refinement, so that each cell is refined into only 2 or 4 smaller cells, instead of into always 8 smaller cells.

**Asked by :** Kevin Maki, University of Michigan

**Answer:** Anisotropic refinement in the way we interpret the question would lead to stretched, non-cubic cells. As shown in Figure 3 (b) in our abstract, this significantly decreases the accuracy of the numerical solution. Moreover, we have experienced in 2D that using significantly stretched cells is detrimental to the stability in a time-integration scheme. We would therefore not recommend such approach.

However, using an anisotropic refinement in the sense that the grid is refined more in certain directions appears promising. In an adaptive scheme, one may e.g. let the refined region be related to the gradient of the velocity.

# Discussion Sheet

**Paper title :** Optimizing wave-generation and -damping in 3D-flow simulations when using implicit relaxation-zones

**Author(s):** R. Perić, V. Vukčević, M. Abdel-Maksoud, H. Jasak

**Question(s) / Comment(s):** I would like to thank you for the clear presenation on your research that I think is very important. I use a very similar technique in my computations, and I relate the time-scale of the relaxation to the time step size. I have found that typically a factor of 10-100 times dt is effective. Can you comment on whether your method relates tau to the time-step size, or the time-scale of the problem of interest?

**Asked by :** Kevin Maki, University of Michigan

**Answer:** Thank you for this question. The optimum value for tau depends on the time-scale of the problem of interest, not on the time-step size.

However, in many flow simulations with free-surface waves, the wave period T determines the time-step size (often T/250 < dt < T/1000). Then, setting tau=X*dt with empirical coefficient X provides the correct scaling of the source term magnitude. So if the same number of time-steps per wave period are used, and if the relaxation zone thickness per wavelength is the same, then the implicit relaxation zone will behave similarly in model scale as in full scale.

Whether a default value of 10*dt < tau < 100*dt is effective depends on which blending function b(x) and which zone thickness x_d are used. Below is the analytical estimate of reflection coefficient C_R as a function of relaxation parameter tau, for a zone thickness of one wavelength, a wave period of T=1.6s and power blending with different exponents n. For T/250 < dt < T/1000, setting 10*dt < tau < 100*dt would result in 0.016s < tau < 0.64s (indicated by a green arrow in the figure). For example, for quadratic blending (i.e. n=2, which would look similar to the curve for n=1, but shifted slightly to the left) the setting tau = 10*dt or tau=100*dt could be anywhere between close-to-optimal or two orders of magnitude smaller than the optimum value, depending on the time-step size. Considering that simulation results for reflection coefficients left of the optimum (i.e. minimum) tau-value can be lower than the analytical prediction, and that increasing the zone thickness increases the range of tau-values which produce satisfactory wave damping, it can be expected for many typical applications from naval hydrodynamics, that your findings for tau will be close to both the analytical and actual optimum value of tau. For the above reasons, tau=X*dt with empirical coefficient X could be a reasonable default-setting.

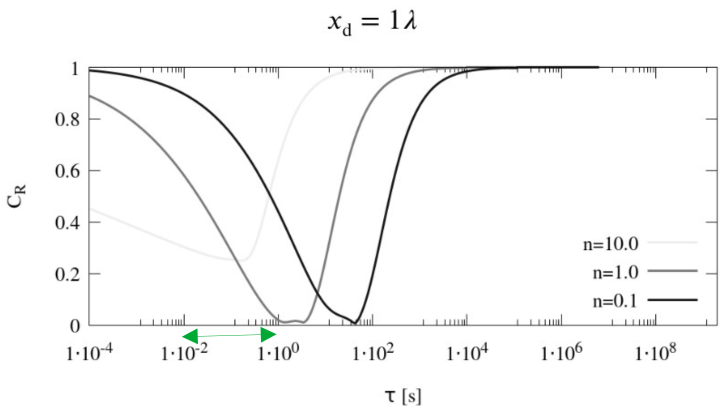


However, a problem with setting tau=X*dt is that, when changing the time-step size, the reflection coefficient of the relaxation zone changes as well. This is because the optimum tau-value depends on the wave period, but not on the time-step.

Thus, when setting tau=X*dt, performing discretization dependence studies is not feasible, because reflection can increase when the time-step is refined. For vanishing time-steps (dt → 0s) holds C_R → 1, i.e. full reflection! For the same reasons, using tau=X*dt with adaptive time-step sizes could result in the relaxation zone becoming suddenly strongly reflective. Furthermore, tau=X*dt can be a problematic choice for flow problems, in which the time-step size is determined not by the waves; for example, flow simulations of ship maneuvers with fully resolved propellers can require much finer time-steps, and consequently the empirical choice for X in tau=X*dt may become inadequate.

*Therefore, optimizing tau and the other parameters of implicit relaxation zones based on the presented analytical approach is recommended.* This enables the use of thinner relaxation zones and increases confidence that wave reflections will be reliably minimized.

For example, the following two figures show analytical estimates of reflection coefficient C_R as a function of relaxation parameter tau and zone thickness x_d, nondimensionalized by the wave period T and the wavelength lambda. The results apply for a quadratic blending function b(x). Similar plots can be generated for any continuous or discontinuous blending function b(x) using the open-source computer code:

https://github.com/wave-absorbing-layers/relaxation-zones-for-free-surface-waves

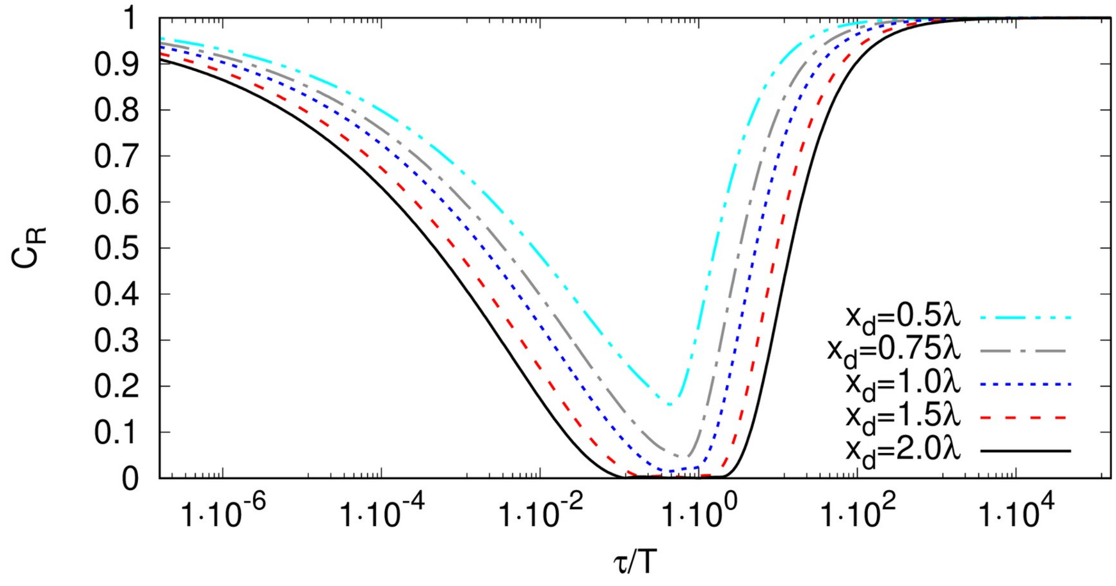

1
0.9
0.8
0.7
0.6
0.5
0.4
0.3
0.2
0.1
0
C_R
1·10^-6
1·10^-4
1·10^-2
1·10^0
1·10^2
1·10^4
τ/T
x_d=0.5λ
x_d=0.75λ
x_d=1.0λ
x_d=1.5λ
x_d=2.0λ


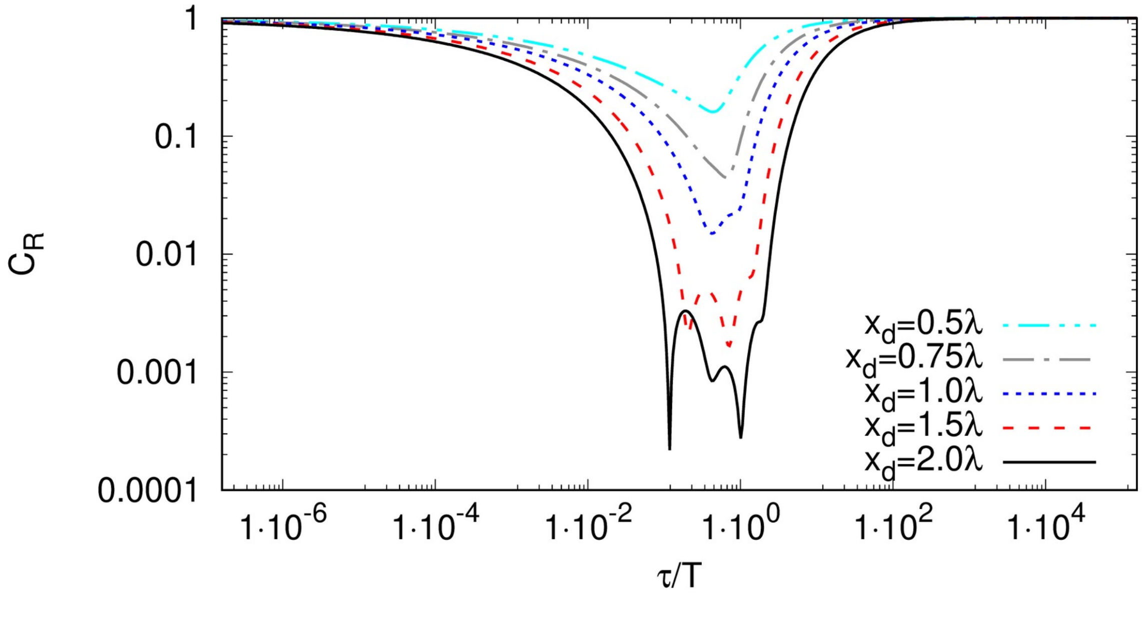

1
0.1
0.01
0.001
0.0001
C_R
1·10^-6
1·10^-4
1·10^-2
1·10^0
1·10^2
1·10^4
τ/T
x_d=0.5λ
x_d=0.75λ
x_d=1.0λ
x_d=1.5λ
x_d=2.0λ

**36th International Workshop on Water Waves and Floating Bodies**

**April 25-28, 2021**

# Discussion Sheet

**Paper title :** A robust mass-momentum flux scheme for simulation of breaking ship waves

**Author(s):** C. Liu, C. Hu, D. Wan

**Question(s) / Comment(s):** Thank you for your paper and presentation with very impressive results and videos. I would like to ask you what is the order-of-accuracy of your method?

**Asked by :** Kevin Maki, University of Michigan

**Answer:**

Dear Prof. Maki,

Thank you very much for your question.
Here is a list of what we are using in our code:
5th order WENO for advection term,
Central differential scheme for diffusion and Laplacian term,
2nd order Adams-Bashforth scheme for time advancing.
PLIC-VOF(or CLSVOF) for tracking the interface.
Sharp surface force model (Mark Sussman) for modeling surface tension.
If you mean the accuracy of mass-momentum consistent method, and if we use a t ypical physical variable (like kinetic energy or mass momentum) to estimate the spa tial convergence rate, then I have to say that the newly developed method will not break the 2nd order convergence rate of original overall accuracy.

Please don't hesitate to ask me for more details about the code.

Thank you very much!
Best regards,

Cheng LIU
2021/5/6

# Discussion Sheet

**Paper title :** Extending limits on wave power absorption by axisymmetric devices
**Author(s):** Porter R., Zheng S., Greaves D.

**Question(s) / Comment(s):**

You show the capture factor for the discrete paddle solution rapidly converging to the continuum case. Is there a connection to other work showing rapid convergence for individual radiating/scattering elements arranged in a ring – e.g. Martin (2014), who showed that the far-field behaviour of a ring of acoustic line sources exhibited exponentially fast convergence towards the 'continuum' solution as the number of sources increased?

Martin, P.A., 2014. On acoustic and electric Faraday cages. Proceedings of the Royal Society A: Mathematical, Physical and Engineering Sciences, 470(2171), p.20140344.

**Asked by :** Hugh Wolgamot (UWA)

**Answer:**

This is not something we have looked at, but I agree it would seem that there could well be such a connection and it would certainly be interesting to explore this further.

# Discussion Sheet

**Paper title : Compound pendulum model of a moored heaving buoy**

**Author(s):** Jana Orszaghova, Hugh Wolgamot, Jørgen Hals Todalshaug, Herve Gaviglio

**Question(s) / Comment(s):** I note that on your contour plots of response as a function of T and H, you show some wave conditions which would be very far from linear, if not beyond the point of wave breaking. From a practical point of view, it would be useful to constrain the plot to realistic values.

**Asked by : Harry Bingham**

**Answer:**

Thank you for pointing this out. In the plots below we have indicated the appropriate range. The solid grey line shows the simple steepness-governed breaking limit given by $H_B = \frac{1}{7}L$, where $H_B$ and $L$ denote the breaking wave height and the wavelength. Conditions violating this limit should be discarded as unphysical. The dashed and the dotted lines represent $0.25\ H_B$ and $0.1\ H_B$. The top left corner of the plots demarcated by the dashed line corresponds to conditions certainly outside the linear range, though at this stage we are unable to comment on the influence of higher-order hydrodynamic terms on the WEC motion responses. Conditions beneath the dotted line should be within the range where linear hydrodynamics works well.

Note that depth-induced breaking does not occur for the 50m water depth and the simulated conditions.

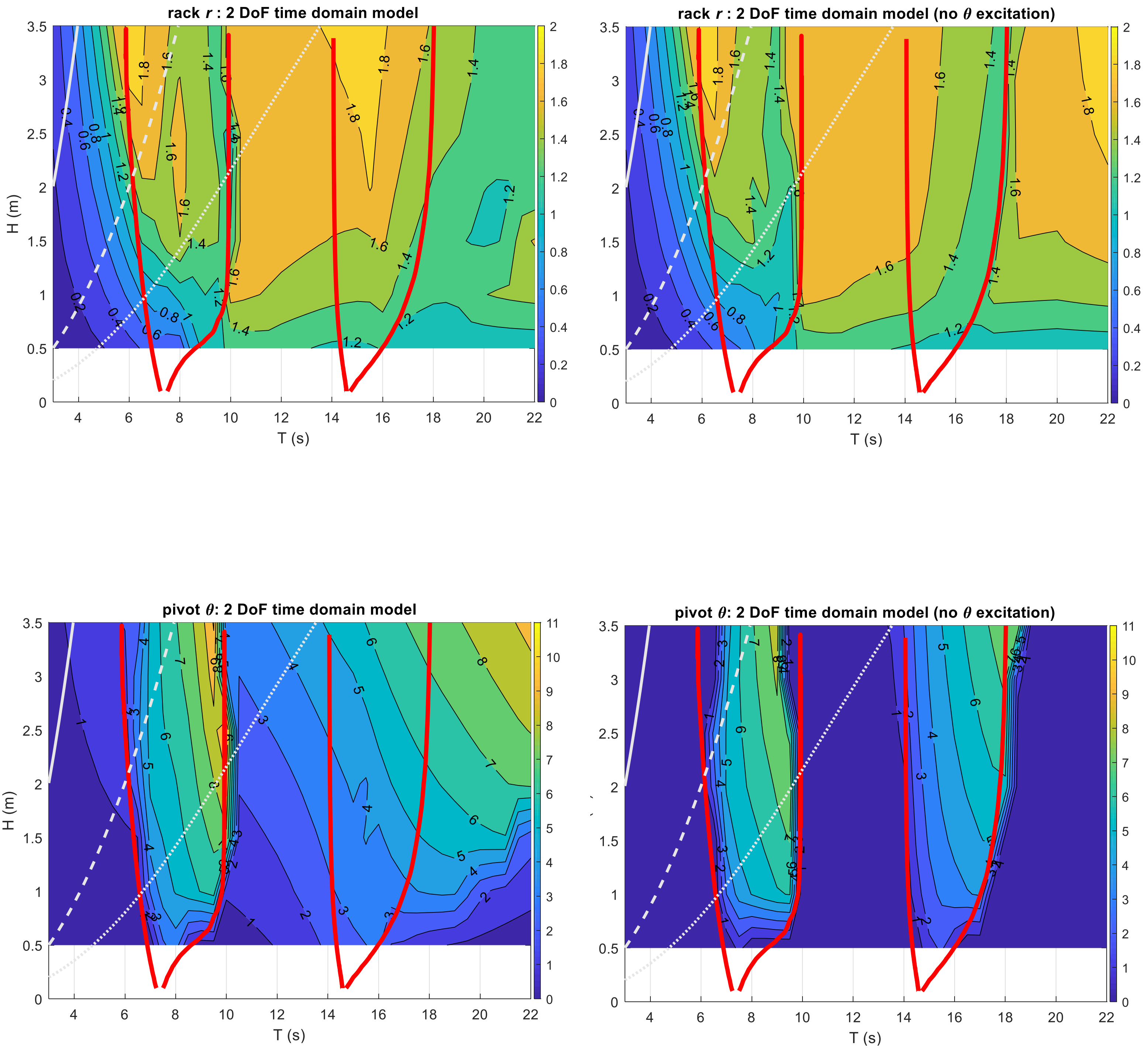

rack r : 2 DoF time domain model
rack r : 2 DoF time domain model (no θ excitation)
pivot θ: 2 DoF time domain model
pivot θ: 2 DoF time domain model (no θ excitation)
H (m)
T (s)

**36th International Workshop on Water Waves and Floating Bodies**

**April 25-28, 2021**

# Discussion Sheet

**Paper title : Compound pendulum model of a moored heaving buoy**

**Author(s): J. Orszaghova, H. Wolgamot, J.H. Todalshaug, H.Gaviglio**

**Question(s) / Comment(s):** If you compare the motion instabilities for this device as compared to other point-absorbers that you have studied; how does the negative spring in the CorPower device affect the likelihood or severity of experiencing Mathieu instabilities?

**Asked by : Malin Göteman**

**Answer:**

From the analysis in this workshop paper and our previous work in [1] and [2], the linear Mathieu equation provides a good prediction for occurrence of instability. The diagram in Figure 1 below shows the stable and unstable regions. It follows that the presence of instability is governed by the amplitude of the parametric excitation (denoted by $\epsilon$) and the amount of linear damping in the unstable mode of motion (denoted by $\mu$). In the point absorber WECs we have studied the parametric excitation was provided through the heave motion. This means that WECs undergoing larger heave motions can develop motion instabilities even in milder wave conditions. The negative spring mechanism in CorPower's device allows for large heave motion across a wide range of wave frequencies, so there is more parametric excitation which can potentially feed into the pendulum mode instability. However, the broad heave motion response is clearly desirable for a heaving WEC. We suspect that the performance of a surface-piercing heaving WEC with a negative spring mechanism would be far superior to an equivalent device without the negative spring, even in the presence of the motion instabilities. However, we have not carried out this direct comparison and leave it as further work.

linear Mathieu equation: $$\ddot{\theta} + 2\mu\dot{\theta} + \Big(\delta + 2\epsilon\cos(2\tau)\Big)\theta = 0$$

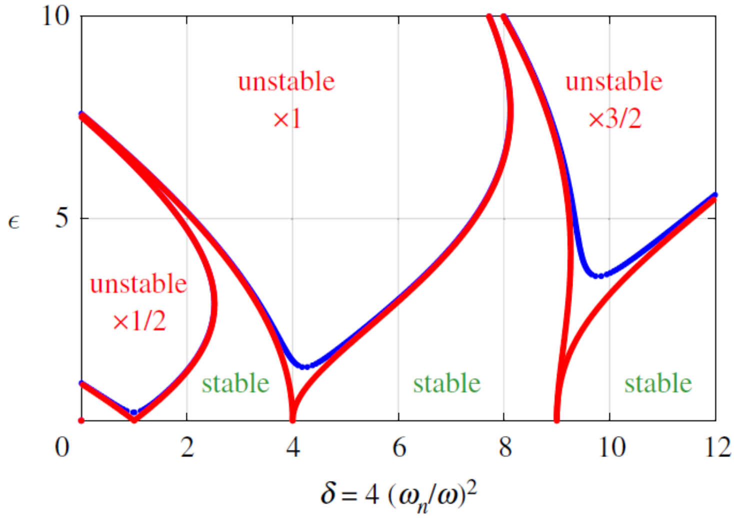


Figure 1: Stability diagram of the linear Mathieu equation. Blue curves correspond to non-dimensional damping μ=0.1, whereas the red curves correspond to an undamped case where μ=0.


[1] Orszaghova, Wolgamot, Draper, Eatock Taylor, Taylor & Rafie, 2019, Transverse motion instability of a submerged moored buoy, Proceedings of the Royal Society A, 475, https://doi.org/10.1098/rspa.2018.0459

[2] Orszaghova, Wolgamot, Draper, Taylor & Rafiee, 2020, Onset and limiting amplitude of yaw instability of a submerged three-tethered buoy, Proceedings of the Royal Society A, 476, https://doi.org/10.1098/rspa.2019.0762